

Power-Minimization under Statistical Delay Constraints for Multi-Hop Wireless Industrial Networks

Neda Petreska, Fraunhofer Institute for Embedded Systems and Communication Technologies ESK
Hussein Al-Zubaidy, School of Electrical Engineering, KTH Royal Institute of Technology
Rudi Knorr, Fraunhofer Institute for Embedded Systems and Communication Technologies ESK
James Gross, School of Electrical Engineering, KTH Royal Institute of Technology

The increased deployment of wireless networks for battery-limited industrial applications in recent years highlights the need for tractable performance analysis and efficient QoS-aware transmit power management schemes. Modern industrial solutions deploy *multi-hop topologies* in order to bridge larger distances without necessarily shortening nodes' battery lifetime. This poses a significant challenge, as multi-hop analysis for *heterogeneous* wireless networks does not exist prior to our work. We overcome this challenge by extending a newly developed methodology based on (\min, \times) network calculus and provide a closed-form expression for the end-to-end delay violation probability over a cascade of heterogeneous buffered wireless fading channels. We further design model-based algorithms for power-minimization and network lifetime maximization which compute the optimal transmit power per node, along a QoS-constrained path. Our numerical study shows an overall transmit power savings of up to 95% when compared to a fixed power allocation. We also apply our algorithm to a realistic WirelessHART network setup and observe that link heterogeneity can significantly influence network lifetime when no efficient power management is applied. This work is especially useful for battery-powered wireless sensor nodes in QoS-constrained applications and offers a solid framework for network design and performance analysis of heterogeneous multi-hop wireless industrial networks.

Additional Key Words and Phrases: stochastic network calculus, wireless sensor networks, multi-hop, heterogeneous networks, end-to-end delay bound, power minimization, industrial networks, WirelessHART

1. INTRODUCTION

In recent years, wireless networking solutions are increasingly being deployed to many new domains such as vehicular networks, machine-to-machine (M2M) communication, home automation, industrial settings and the smart grid. Applications in these areas often require novel combinations of delay and reliability constraints, while on the other hand relying on battery-driven wireless systems. One area where these aspects are especially important is the area of wireless industrial networks, in particular, process automation. Process automation comprises the area of process sensing, control and diagnostics. Target application areas can be found, for example, in refineries, food and chemical industries. Typical process automation applications have Quality-of-Service (QoS) demands with deadlines in the order of hundreds of milliseconds and maximum outage probabilities (with respect to the deadlines) in the order of 10^{-3} to 10^{-4} [ZVEI - German Electrical and Electronic Manufacturers' Association 2009]. At the same time, these applications correspond to processes span over quite a wide range of distances, varying from few meters up to few kilometers. Battery-driven wireless sensors and actuators are mainly applied in these scenarios due to their flexible placement possibilities. For larger distances, this usually leads to multi-hop networking in order to avoid high transmit powers draining the battery and thus shortening the lifetime of the network. In addition, it is well known that dynamic transmit power management, being one of the main energy consumers in a wireless device [Berry 2013], has the potential in such scenarios to improve battery lifetime in addition to other techniques, such as hardware design, load balancing and transceiver state transition [Zheng and Kravets 2005].

Nevertheless, when it comes to dependable industrial and machine-to-machine applications, transmit power management is challenging as it has to factor in latency and reliability constraints. This necessitates a trade-off between power consumption

at each node and the physical channel transmit rate, which potentially leads to a queue build-up at that node. Although transmit power management under QoS requirements has been addressed for single-hop communications [Berry 2013; Zafer and Modiano 2005; Tang and Zhang 2008a; Kandukuri and Boyd 2002], power management under a stochastic queuing constraint for multi-hop networks remains to date an open problem. In the following, we discuss related work with respect to general end-to-end transmit power management schemes, before we address works that deal with multi-hop end-to-end queuing performance.

Power management under *simplified* end-to-end throughput constraints has been often addressed before [Kozat et al. 2006; Cruz and Santhanam 2003; Katsenou et al. 2013; Banerjee and A. 2002; Julian et al. 2002]. However, none of these works considers queuing effects. For instance, [Kozat et al. 2006] describes a cross-layer design framework, minimizing the total transmit power subject to a minimal end-to-end payload rate valid for all links and maximal bit error rate (BER) requirements per session. The authors use heuristics to determine the transmit power per node. [Cruz and Santhanam 2003] minimizes the total average transmit power under the constraint of providing a minimum average data rate per link. The authors propose an algorithm for optimal link scheduling and power control policy. They also extend this to a routing algorithm, which uses the algorithms output as routing metric. They show that the optimal power policy chooses one of two actions, transmitting at peak power or not transmitting at all. Transmit power control in multi-hop networks with respect to the best possible video quality at the receiver is presented in [Katsenou et al. 2013]. For this purpose, the authors maximize the peak signal-to-noise ratio and minimize the end-to-end video distortion, which is a function of the end-to-end bit error probability. Results show that power control does not degrade video quality significantly. With respect to power management and end-to-end multi-hop performance, two works are perhaps closest to our contribution. First, [Tang and Zhang 2008b] presents a trade-off between the average transmit power and a corresponding queuing-delay bound for a multiuser cellular network, multi-hop and point-to-point communication. The authors propose a resource allocation scheme to minimize power consumption subject to statistical delay QoS, given as a queue-length decay rate, jointly determined from the effective bandwidth of the arrival traffic and the effective capacity of the wireless channel. The numerical analysis show that it is possible to achieve stringent QoS guarantee with little power increase compared to the power needed for loose delay constraints. However, the discussed multi-hop scenario assumes an amplify-and-forward scheme, and therefore does not consider queuing at the intermediate nodes. Second, in [Neely et al. 2005] the authors present a joint routing and power allocation policy for a wireless multi-hop network with time-varying channels that stabilizes the system and provides bounded average delay guarantees. The optimal power allocation in both proposed schemes, defined as distributed and centralized control algorithm, is determined under pre-defined stability condition, i.e., for input rates which are strictly inside the network capacity region. It is shown that the derived delay bounds grow asymptotically in the size of the network and a parameter that describes the distance between the arrival rates and the capacity region boundary. The numerical results illustrate the advantage of exploiting channel state and queue backlog. The work, however, covers queuing by focusing mainly on a stability condition and does not consider quantiles on the end-to-end delay.

From a queuing-theoretic perspective, significant problems arise when trying to characterize such quantiles on the end-to-end delay performance of a wireless multi-hop network. Classical models for queuing networks typically only allow the analysis of the average delay. In contrast, the theory of network calculus enables an analysis of delay quantiles via bounds on the arrival and service rather than focusing on the

average behaviour. In particular, stochastic network calculus [Jiang and Liu 2008] has shown to be especially useful for characterizing traffic arrivals and network service guarantees over wireless fading channels using this theoretical framework [Jiang and Emstad 2005b; Fidler 2006a; Lubben and Fidler 2012; Fidler 2006b; Ciucu et al. 2010; Ciucu 2011; Ciucu et al. 2014; Ciucu et al. 2005], none of them resolve the question on end-to-end delay bounds over heterogeneous fading channels. Attempts in that direction are presented in [Ciucu et al. 2010] and [Fidler 2006a]. However, while the first one does not provide a closed-form expression for the end-to-end service curve for wireless fading channels, the complexity of the MGF-based framework presented in [Fidler 2006a] grows very fast when considering a multi-hop path and results in mathematically intractable expressions. Furthermore, the usage of the Gilbert-Elliott two-state channel model in [Fidler 2006b] limits the accuracy of the fading model description.

A recently developed theoretical framework has enabled an analytical toolset for performance analysis of wireless multi-hop fading channels [Al-Zubaidy et al. 2013]. By means of (\min, \times) -calculus, bounds on the delay and the backlog are expressed in terms of fading channel gain distribution, working directly in the so called signal-to-noise ratio (SNR) domain. In this domain, multi-hop descriptions of fading channels become mathematically tractable. Based on this work, we have made first attempts to determine the minimal required SNR on a single link in order to meet pre-defined statistical delay requirements [Petreska et al. 2014]. However, [Al-Zubaidy et al. 2013] addresses only independent and identically distributed (i.i.d.) wireless channel gains, which limits the applicability of the results to general scenarios. We have therefore extended the proposed framework for non-identically distributed channel gains and, together with the above mentioned power- and QoS-based issues, present in this paper the following contributions:

- A closed-form expression for the end-to-end delay violation probability over a wireless multi-hop path consisting of independent, but non-identically distributed channel gains is derived. Our formulation reveals a recursive nature of the end-to-end service and delay bound and provides important insights on the statistical delay in fading networks [Petreska et al. 2015].
- An iterative delay-aware power-minimization algorithm for wireless multi-hop heterogeneous networks with two variations: minimizing the total transmit power along the path and maximizing the network lifetime.
- Numerical evaluation presenting the advantage of using the proposed algorithms in comparison to a fixed transmit power scheme.

The obtained results for power gain (using Shannon-based capacity) and network lifetime extension (assuming an IEEE 802.15.4-based link capacity) offer significant insights into multi-hop network design, considering thereby both link and battery charge-state heterogeneity.

The paper is organized as follows: Section 2 presents the system model and the problem statement. In Section 3 we present the closed-form of the end-to-end delay bound for heterogeneous wireless networks. These results are the basis for the power minimization algorithms discussed in Section 4. We validate our analytical findings in Section 5, which also contains the discussion on numerical results. Finally, Section 6 concludes the paper.

2. SYSTEM MODEL AND PROBLEM STATEMENT

We consider the communication between a source node r and a destination node d within a multi-hop wireless network (see Fig. 1). Let the multi-hop path in question, illustrated with the solid lines in Fig. 1, be given with an ordered set of buffered links,

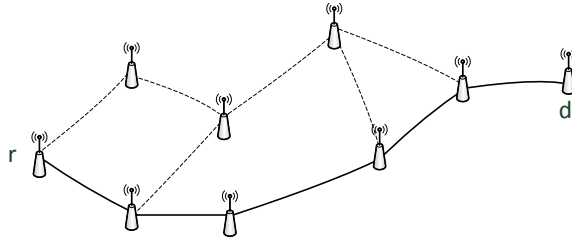


Fig. 1: Illustration of the system model

i.e., $\mathbb{L} = \{1, \dots, N\}$, where N is the number of links constituting path \mathbb{L} . We assume a time-slotted system where every link is assigned a time slot of fixed-length T in a round-robin fashion. During each slot, packets of fixed size r_a are forwarded by the respective node over the next hop to the corresponding receiver along the path. As soon as the packet reaches the destination node, it is passed to its application layer without any additional delay. Therefore, the minimal delay a packet experiences on the path is $N \cdot T$.

Each wireless link $n \in \mathbb{L}$ is assumed to be a block-fading channel with average channel gain $|\bar{h}_n^2|$. This means, the random instantaneous channel gain $h_{i,n}^2$ of link n at time slot i remains constant within the time interval T , but varies independently from slot to slot. Different links are assumed to have statistically independent channel gains while in general we consider non-identically distributed channel gains. Moreover, the instantaneous channel gain consists of two components: the instantaneous fading component h_f^2 and the constant path-loss h_p^2 , the latter depending on the distance between the nodes and the path-loss exponent, i.e., $h_{i,n}^2 = h_{f,i,n}^2 \cdot h_{p,n}^2$. Interference is not considered in the paper. Together with the transmit power setting $p_{i,n}$ and the noise power σ^2 , this yields the instantaneous SNR of link n in time slot i as:

$$\gamma_{i,n} = \frac{p_{i,n} \cdot h_{i,n}^2}{\sigma^2} \quad (1)$$

Given the instantaneous SNR $\gamma_{i,n}$, the resulting service per link n is given by the link's capacity at time slot i . We denote the capacity of link n during time slot i by the function $g(\gamma_{i,n})$. We assume that only n 's average channel state information $|\bar{h}_n^2|$, but not the instantaneous one, $h_{i,n}^2$, is known at the transmitter. Furthermore, we define $\vec{\gamma}$ and \vec{p} as the vectors of average SNRs and transmit power of the links, i.e., nodes along the path, respectively.

At the application layer, we consider a monitoring process generating a measurement value at a regular interval. Therefore, as a model for the arrival flow we consider packets of size r_a bits arriving per interval $\beta \cdot T$ with $\beta \in \mathbb{N}$. However, the application has strict latency and reliability constraints. These are modeled by the QoS pair $\{\omega^\varepsilon, \varepsilon\}$ where ω^ε represents a maximum tolerable delay while ε represents a violation probability with respect to ω^ε . This delay target includes all processing steps below the application layer, therefore including also any queuing delay along the multi-hop path.

In this paper, we are interested in the trade-off between the energy consumption of the network - mainly driven by the transmit power per node $p_{i,n}$ - and the resulting delay and delay violation probability. In this context, we are in particular interested in the minimization of the sum of the transmit power along the path (in the following referred to as *total transmit power*) under given QoS pair $\{\omega^\varepsilon, \varepsilon\}$ or in the maximization of the network lifetime given a battery state vector \vec{B} consisting of battery states per

node ¹, B_n , as well as an energy consumption model, under a given QoS pair $\{\omega^\varepsilon, \varepsilon\}$. In the following, we will develop algorithms that determine the corresponding network configurations (i.e., transmit power settings) under the mentioned constraints. However, in order to invoke those algorithms, the first step is to develop an analytical model of the end-to-end delay performance in a wireless multi-hop network under a given transmit power configuration. We first approach this problem in the next section, and then present the algorithms for total power minimization and network lifetime maximization in Sec. 4.

3. END-TO-END DELAY BOUND OVER HETEROGENEOUS LINKS

In this section, we develop end-to-end performance bounds based on stochastic network calculus for heterogeneous multi-hop paths. So far, in the context of wireless fading channels, end-to-end probabilistic bounds have only been obtained for concatenated i.i.d. service processes (i.e., for multi-hop wireless links all having independent and identically distributed fading processes) [Al-Zubaidy et al. 2013]. In order to apply these results to heterogeneous networks, we generalize the available results to arbitrarily distributed random service processes. For reader's benefit, we first recap some network calculus basics before presenting our theorem.

3.1. Stochastic Network Calculus

Stochastic network calculus considers queuing systems and networks of systems with stochastic arrival and departure processes, where the bivariate functions $A(\tau, t)$, $D(\tau, t)$ and $S(\tau, t)$ for any $0 \leq \tau \leq t$ denote the *cumulative* arrivals to the system, departures from the system, and service offered by the system, respectively, in the interval $[\tau, t)$. Recall that we consider a discrete time model, where time slots have a duration T and $i \geq 0$ denotes the index of the respective time-slot.

A lossless system with service process $S(\tau, t)$ satisfies the input/output relationship $D(0, t) \geq A \otimes S(0, t)$, where \otimes is the $(\min, +)$ convolution operator given by

$$x \otimes y(\tau, t) = \inf_{\tau \leq u \leq t} \{x(\tau, u) + y(u, t)\} . \quad (2)$$

As stated above, in general we are interested in probabilistic bounds of the form $\Pr[W(t) > w^\varepsilon] \leq \varepsilon$, which is also known as the *violation probability* for a target delay w^ε , under the following system stability condition:

$$\lim_{t \rightarrow \infty} \frac{A(0, t)}{t} < \lim_{t \rightarrow \infty} \frac{S(0, t)}{t} . \quad (3)$$

Modeling wireless links in the context of network calculus however is not a trivial task. A particular difficulty arises when we seek to obtain a stochastic characterization of the cumulative service process of a wireless fading channel, as also witnessed in the context of the effective service capacity of wireless systems [Wu and Negi 2003]. A promising, recent approach for wireless networks has been proposed in [Al-Zubaidy et al. 2013] where the queuing behavior is analyzed directly in the “domain” of channel variations instead of the bit domain [Jiang and Emstad 2005a; Fidler 2006b; Lee and Jindal 2009; Mahmood et al. 2011; Fidler 2006a; Wu and Negi 2003]. This can be interpreted as the *SNR domain* (thinking of bits as “SNR demands” that reside in the system until these demands can be met by the channel).

To start with, the cumulative arrival, service, and departure processes in the bit domain, i.e., A , D , and S , are related to their SNR domain counterparts (represented in the following by calligraphic capital letters \mathcal{A} , \mathcal{D} , and \mathcal{S}) respectively, through the

¹In order to simplify the notation, we refer to node n as the node preceding link n .

exponential function. Thus, we have $\mathcal{A}(\tau, t) \triangleq e^{A(\tau, t)}$, $\mathcal{D}(\tau, t) \triangleq e^{D(\tau, t)}$, and $\mathcal{S}(\tau, t) \triangleq e^{S(\tau, t)}$. Due to the exponential function, these cumulative processes become products of the increments in the bit domain. In the following, we will assume $\mathcal{A}(\tau, t)$ and $\mathcal{S}(\tau, t)$ to have stationary and independent increments. We denote them by α for the arrivals (in SNR domain) and $g(\gamma)$ for the service. For instance, assuming a single-hop wireless system where the SNR domain is related to the bit domain through the well-known Shannon capacity expression, we write:

$$s_i = \log(g(\gamma_i)) = C \log_2(1 + \gamma_i), \quad (4)$$

where s_i is the random service in bits offered by the system in time slot i , C is the number of transmitted symbols per time slot, and γ_i is the instantaneous SNR. Then, we can obtain the cumulative service process in the SNR domain as

$$\mathcal{S}(\tau, t) = \prod_{i=\tau}^{t-1} e^{s_i} = \prod_{i=\tau}^{t-1} g(\gamma_i) = \prod_{i=\tau}^{t-1} (1 + \gamma_i)^C, \quad (5)$$

where $C = C/\log 2$. Furthermore, in case of first-come first-served order, the delay at time t is obtained as follows

$$W(t) = \mathcal{W}(t) = \inf\{i \geq 0 : \mathcal{A}(0, t)/\mathcal{D}(0, t+i) \leq 1\}. \quad (6)$$

A bound ε for the delay violation probability $\Pr[W(t) > w^\varepsilon]$ can be derived based on a transform of the cumulative arrival and service processes in the SNR domain using the moment bound. In [Al-Zubaidy et al. 2013], it was shown that such a violation probability bound for a given w^ε can be obtained as $\inf_{s>0} \{\mathcal{K}(s, t + w^\varepsilon, t)\}$. We refer to the function $\mathcal{K}(s, \tau, t)$ as the *kernel* defined as

$$\mathcal{K}(s, \tau, t) = \sum_{i=0}^{\min(\tau, t)} \mathcal{M}_{\mathcal{A}}(1 + s, i, t) \mathcal{M}_{\mathcal{S}}(1 - s, i, \tau), \quad (7)$$

where the function $\mathcal{M}_{\mathcal{X}}(s)$ is the Mellin transform [Davies 1978] of a random process, defined as

$$\mathcal{M}_{\mathcal{X}}(s, \tau, t) = \mathcal{M}_{\mathcal{X}(\tau, t)}(s) = \mathbb{E}[\mathcal{X}^{s-1}(\tau, t)], \quad (8)$$

for any $s \in \mathbb{C}$, whenever the expectation exists (we restrict our derivations in this work to real valued $s \in \mathbb{R}$).² Introducing the Mellin transform in the performance analysis of wireless fading channels results into tractable mathematical expressions when computing network calculus bounds, which in turn results in scalable closed-form solutions. The Mellin transforms become independent of the time instance, and we write $\mathcal{M}_{\mathcal{X}}(s, t - \tau)$. In addition, as we only consider stable queuing systems in steady-state, the kernel becomes independent of the time instance t and we denote $\mathcal{K}(s, t + w^\varepsilon, t) \stackrel{t \rightarrow \infty}{\rightleftharpoons} \mathcal{K}(s, -w^\varepsilon)$.

The strength of the Mellin-transform-based approach becomes apparent when considering block-fading channels. The Mellin transform for the cumulative service process in SNR domain is given by

$$\mathcal{M}_{\mathcal{S}}(s, \tau, t) = \prod_{i=\tau}^{t-1} \mathcal{M}_{g(\gamma)}(s) = \mathcal{M}_{g(\gamma)}^{t-\tau}(s) = \mathcal{M}_{\mathcal{S}}(s, t - \tau),$$

²We note that by definition of $\mathcal{X}(\tau, t) = e^{X(\tau, t)}$, the Mellin transform $\mathcal{M}_{\mathcal{X}}(s, \tau, t) = \mathbb{E}[e^{(s-1)X(\tau, t)}]$ after substitution of parameter $s = \theta + 1$ implies also a solution for the moment-generating function (MGF), that is the basis of the effective capacity model [Wu and Negi 2003] and of an MGF network calculus [Fidler 2006a].

where $\mathcal{M}_{g(\gamma)}(s)$ is the Mellin transform of the stationary and independent service increment $g(\gamma)$ in the SNR domain. The function $g(\cdot)$ represents here the channel capacity, of a point-to-point fading channel as given by Eq. (4). However, it can also model more complex system characteristics, most importantly scheduling effects.

Assuming the cumulative arrival process in SNR domain to have stationary and independent increments we denote the corresponding Mellin transform by $\mathcal{M}_A(s, t - \tau) = \prod_{i=\tau}^{t-1} \mathcal{M}_\alpha(s) = \mathcal{M}_\alpha^{t-\tau}(s)$. Substituting these two cumulative processes in Eq. (7), for the steady-state kernel for a fading wireless channel we get [Petreska et al. 2014]

$$\mathcal{K}(s, -w) = \frac{\mathcal{M}_{g(\gamma)}^w(1-s)}{1 - \mathcal{M}_\alpha(1+s)\mathcal{M}_{g(\gamma)}(1-s)} \quad (9)$$

for any $s > 0$, under the stability condition

$$\mathcal{M}_\alpha(1+s)\mathcal{M}_{g(\gamma)}(1-s) < 1. \quad (10)$$

Assuming Rayleigh fading, i.e., an exponentially distributed SNR with average $\bar{\gamma}$ at the receiver, the Mellin transform of the service process results into [Al-Zubaidy et al. 2013]

$$\mathcal{M}_{g(\gamma)}(s) = e^{\frac{1}{\bar{\gamma}}\bar{\gamma}^{s-1}}\Gamma\left(s, \bar{\gamma}^{-1}\right). \quad (11)$$

where $\Gamma(x, y) = \int_y^\infty t^{x-1}e^{-t}dt$ is the incomplete Gamma function. Then the steady-state kernel for a Rayleigh-fading wireless channel turns out to be:

$$\mathcal{K}(s, -w) = \frac{\left(e^{1/\bar{\gamma}}\bar{\gamma}^{-s}\Gamma\left(1-s, \frac{1}{\bar{\gamma}}\right)\right)^w}{1 - \mathcal{M}_\alpha(1+s)e^{1/\bar{\gamma}}\bar{\gamma}^{-s}\Gamma\left(1-s, \frac{1}{\bar{\gamma}}\right)} \quad (12)$$

for any $s > 0$ and under the stability condition in Eq. (10). By substituting Eq. (12) in $\inf_{s>0}\{\mathcal{K}(s, -w)\}$, a bound on the delay violation probability $\varepsilon(w)$ for a given w can be obtained.

3.2. Recursive Formula

A very important strength of network calculus is the ability to capture a concatenated service process into a so called joint service curve. This property is especially useful for performance analysis of multi-hop networks. Similarly to the $(\min, +)$ algebra, the joint service curve is obtained through the end-to-end convolution according to the (\min, \times) network calculus and for a path \mathbb{L} it is defined as follows:

$$\mathcal{S}_{\mathbb{L}}(\tau, t) = \mathcal{S}_1 \otimes \mathcal{S}_2 \otimes \dots \otimes \mathcal{S}_n(\tau, t), \quad (13)$$

where $\mathcal{S}_1 \otimes \mathcal{S}_2(\tau, t) = \inf_{\tau < i \leq t} \{\mathcal{S}_1(\tau, i) \cdot \mathcal{S}_2(i, t)\}$. In the following, we define a bound on the Mellin transform of the end-to-end service considering the following relationship. Let $\mathcal{S}_1(\tau, t)$ and $\mathcal{S}_2(\tau, t)$ be two independent non-negative bivariate random processes representing the service processes of link 1 and 2, respectively. For $s < 1$, the Mellin transform of the (\min, \times) convolution of \mathcal{S}_1 and \mathcal{S}_2 , denoted by $\mathcal{S}_1 \otimes \mathcal{S}_2(\tau, t)$, is bounded by

$$\mathcal{M}_{\mathcal{S}_1 \otimes \mathcal{S}_2}(s, \tau, t) \leq \sum_{i=\tau}^t \mathcal{M}_{\mathcal{S}_1}(s, \tau, i) \cdot \mathcal{M}_{\mathcal{S}_2}(s, i, t)$$

Hence, the corresponding Mellin transform of the path \mathbb{L} can be bounded by [Al-Zubaidy et al. 2013]:

$$\begin{aligned} \mathcal{M}_{S^{\mathbb{L}}}(s, \tau, t) &\leq \sum_{i_1=i_0}^t \sum_{i_2=i_1}^t \cdots \sum_{i_{N-1}=i_{N-2}}^t \mathcal{M}_{S_1}(i_1 - i_0) \cdot \\ &\mathcal{M}_{S_2}(i_2 - i_1) \cdots \mathcal{M}_{S_N}(i_N - i_{N-1}) = \\ &\sum_{i_1 \dots i_{N-1}}^t \prod_{n=1}^N \mathcal{M}_{S_n}^{i_n - i_{n-1}}(s), \end{aligned} \quad (14)$$

with $\tau = i_0 \leq i_1 \leq \dots \leq i_N = t$. Notice that $\mathcal{M}_{S_n}(s)$ denotes the Mellin transform of the (stationary) SNR domain service increment of link n .

As one may notice from Eq. (14), this results in a cumbersome computation, especially for links having different channel gain distribution, since N convolution processes have to be computed, each of them depending on t . Hence, we now present a significant simplification of Eq. (14) into a mathematically easier-to-grasp analytical solution, avoiding the tedious task of performing N convolution operations. For this reason we define $\mathcal{K}^{\mathbb{L}}$ as the kernel for a path \mathbb{L} containing N links, similar to Eq. (7), where we replace $\mathcal{M}_S(1-s, i, \tau)$ with $\mathcal{M}_{S^{\mathbb{L}}}(1-s, i, \tau)$ for $S^{\mathbb{L}}$ defined in Eq. (13). Once that Mellin transform can be determined, the delay bound can be computed using Eq. (7) as follows:

LEMMA 3.1. *For a path \mathbb{L} a probabilistic end-to-end delay bound is given by the minimum w^ε that satisfies*

$$\inf_{s \geq 0} \{ \mathcal{K}^{\mathbb{L}}(s, -w^\varepsilon) \} \leq \varepsilon.$$

Based on this relationship, we present here the first core contribution of our work, representing the first closed-form solution for the computation of the end-to-end delay bound over path \mathbb{L} built of heterogeneous wireless links. Let n and $m \in \{1, 2, \dots, N-1\}$ refer to the n^{th} and the m^{th} link of path \mathbb{L} , respectively.

THEOREM 3.2. *Given a path $\mathbb{L} \setminus \{n\}$ of links with independent and non-identically distributed service processes, with kernel $\mathcal{K}^{\mathbb{L} \setminus \{n\}}$; then $\mathcal{K}^{\mathbb{L}}$ can be obtained in terms of $\mathcal{K}^{\mathbb{L} \setminus \{n\}}$ as follows*

$$\begin{aligned} \mathcal{K}^{\mathbb{L}}(s, -w) &= \\ &= \frac{\mathcal{M}_{g(\gamma_n)}(1-s)}{\mathcal{M}_{g(\gamma_n)}(1-s) - \mathcal{M}_{g(\gamma_m)}(1-s)} \mathcal{K}^{\mathbb{L} \setminus \{m\}}(s, -w) \\ &+ \frac{\mathcal{M}_{g(\gamma_m)}(1-s)}{\mathcal{M}_{g(\gamma_m)}(1-s) - \mathcal{M}_{g(\gamma_n)}(1-s)} \mathcal{K}^{\mathbb{L} \setminus \{n\}}(s, -w) \end{aligned}$$

for any $m \in \{1, 2, \dots, N-1\}$.

The proof of the theorem is given in Appendix A.

A direct consequence of Theorem 3.2 and Lemma 3.1 is that the delay bound for path \mathbb{L} can be obtained from recursively computing the kernel according to the theorem. In this recursion, the number of summands increases with the number of hops. For an N -hop path there are 2^{N-1} summands, as each geometric sum results into two summands. Furthermore, the stability condition in Eq. (10) needs to hold for every individual link $n \in \{1, \dots, N\}$, i.e.,:

$$\max_n (\mathcal{M}_\alpha(1+s) \cdot \mathcal{M}_{g(\gamma_n)}(1-s)) < 1$$

has to be fulfilled.

The proof given in the appendix shows that the recursion obtained for the end-to-end delay bound results from the recursion in the Mellin transform of the joint service curve. In other words, the stepwise construction of a multi-hop path's service curve will further simplify the computation of other elements in (\min, \times) network calculus, such as the delay bound. We demonstrate this by providing the leftover service curve for the considered path when cross-traffic is present, i.e., interfering flows other than $A(\tau, t)$ are sharing the intermediate links in the path that the through flow traverses. Let the SNR arrival processes of the cross traffic at each intermediate link be i.i.d. and denoted by $\mathcal{A}_c(\tau, t) = e^{k_c(t-\tau)}$, where we assume a constant arrival rate of k_c bits per time slot. Assume further that the arrivals from the original through flow and the cross traffic as well as the service processes at each link are independent. We can then compute a bound on the Mellin transform of the end-to-end service process offered to the through flow, i.e., the *leftover service curve* using the following lemma:

LEMMA 3.3. *Consider a flow traversing a cascade of wireless fading channels. The service at each node is shared by the through flow and an independent cross flow characterized by the SNR arrival process $\mathcal{A}_c(\tau, t)$. Let $S_c^{\mathbb{L}}(\tau, t)$ denote the end-to-end leftover service rendered to the through flow. Then, $\forall s < 1$,*

$$\begin{aligned} \mathcal{M}_{S_c^{\mathbb{L}}}(s, \tau, t) \leq & \left(\frac{\mathcal{M}_{g(\gamma_m)}(s)}{\mathcal{M}_{g(\gamma_m)}(s) - \mathcal{M}_{g(\gamma_m)}(s)} \cdot \mathcal{M}_{S_c^{\mathbb{L} \setminus \{m\}}}(s, \tau, t) \right) + \\ & \left(\frac{\mathcal{M}_{g(\gamma_m)}(s)}{\mathcal{M}_{g(\gamma_m)}(s) - \mathcal{M}_{g(\gamma_m)}(s)} \cdot \mathcal{M}_{S_c^{\mathbb{L} \setminus \{n\}}}(s, \tau, t) \right), \end{aligned} \quad (15)$$

for any $m \in \{1, 2, \dots, N-1\}$ and $\mathcal{M}_{S_c^{\{1\}}}(s, \tau, t) = (e^{k_c(1-s)} \cdot \mathcal{M}_{g(\gamma_1)}(s))^{t-\tau}$.

PROOF. According to *Lemma 1* in [Al-Zubaidy et al. 2013] we obtain the Mellin transform of the leftover service curve for a single channel:

$$\begin{aligned} \mathcal{M}_{S_c^{\{1\}}}(s, \tau, t) &= \mathcal{M}_{s/\mathcal{A}_c}(s, \tau, t) \\ &= \mathcal{M}_{g(\gamma_1)}(s, \tau, t) \cdot \mathcal{M}_{\mathcal{A}_c}(2-s, \tau, t) \\ &\leq \left(e^{k_c(1-s)} \cdot \mathcal{M}_{g(\gamma_1)}(s) \right)^{t-\tau}, \end{aligned} \quad (16)$$

since the Mellin transform of a quotient of two independent random variables X and Y is given by $\mathcal{M}_{X/Y}(s) = E[X^{s-1}]E[Y^{1-s}] = \mathcal{M}_X(s) \cdot \mathcal{M}_Y(2-s)$.

Substituting $e^{k_c(1-s)}\mathcal{M}_{g(\gamma_m)}(s)$ for $\mathcal{M}_{g(\gamma_m)}$, $n \in \{1, \dots, N\}$ in the joint service curve derivation given in Appendix A, the expression given by Eq. (15) follows by applying the recursion to the leftover service curve of path \mathbb{L} , $\mathcal{M}_{S_c^{\mathbb{L}}}(s, \tau, t)$. \square

4. POWER MINIMIZATION ALGORITHM

As already mentioned, an essential aspect of industrial wireless networks, besides the importance of QoS-awareness, is their energy-efficient operation. Especially for battery-powered network devices, often attached to machines in order to control them or measure their functional status, it is important to prolong network partitioning time by extending nodes' battery lifetime. Since the radio chip is usually one of the largest consumers of energy in low-power networks [Khader and Willig 2013], one way of providing energy efficiency is to minimize the transmit power, as one of the easily modifying parameters in wireless transceivers. In addition, minimizing transmit power not only increases energy savings, but also reduces potential interference to neighboring transmissions. In a multi-hop setting, power optimization mainly needs to take two

issues into account. On the one hand, heterogeneous link statistics can be exploited to reduce power consumption. On the other hand, heterogeneous battery states affect the transmit power setting. Thus, in this section we develop and present algorithms that take these effects into account in order to minimize transmit power or maximize network lifetime under statistical end-to-end constraints as discussed above.

4.1. Transmit Power Minimization Algorithm

We initially raise the following question: What is the optimal average SNR, i.e., minimal sum transmit power needed on all links along a path to meet the target end-to-end delay w^ε with probability $1 - \varepsilon$? More formally, we are interested in the solution of the following optimization problem for a given multi-hop path $\mathbb{L} = \{1, \dots, N\}$:

$$\begin{aligned} \min \quad & \sum_{n=1}^N p_n, \\ \text{s. t.} \quad & \inf\{s > 0 : \mathcal{K}^{\mathbb{L}}(s, -w^\varepsilon)\} \leq \varepsilon \\ & \max_n (\mathcal{M}_\alpha(1+s) \cdot \mathcal{M}_{g(\gamma_j)}(1-s)) < 1. \end{aligned}$$

Due to the complexity of the kernel function and the stability condition (see Eq. (12)), no analytical solution for the optimal SNR can be derived. Instead, we propose a binary search algorithm in two dimensions (along $s > 0$ and along the average SNR $\bar{\gamma}$) to solve the given minimization problem (see Algorithm 2 in Appendix B). Notice that minimizing $\bar{\gamma}$ leads to minimization of the transmit power per hop, since $\bar{\gamma} = p/\sigma^2$.

The proposed algorithm results in global minimum when the kernel described by Theorem 3.2 is convex in $s > 0$. The following theorem states this (the proof is given in Appendix C):

THEOREM 4.1. *The kernel $\mathcal{K}(s, -w)$ in Eq. (9) is convex in $s, \forall s > 0$.*

Using Theorem 4.1, we show the following:

COROLLARY 4.2. *The end-to-end kernel $\mathcal{K}^{\mathbb{L}}(s, -w)$ is convex in $s, \forall s > 0$.*

PROOF. Theorem 3.2 defines $\mathcal{K}^{\mathbb{L}}(s, -w)$ in terms of a recursion starting with the single hop kernel which is convex in s according to Theorem 4.1. As $\mathcal{M}_{g(\gamma)}(1-s) > 0, \forall s > 0$, the theorem follows since *any positive linear combination of convex functions is also convex* [Clarke 2013]. \square

Figure 2 illustrates the kernel of several links with different average SNR, where the instantaneous channel capacity is given by Eq. (4). The figure shows that, the delay bound function of a single link $\mathcal{K}(s, -w)$ is convex in s and monotone in $\bar{\gamma}$ (block-fading wireless link with constant arrival rate and random service increments that are characterized by the Shannon capacity). We further notice that, as the SNR either increases or decreases, the optimal s^* (which minimizes the delay bound function) moves to the right or to the left, respectively.

For any given transmit power vector $\vec{p} = \{p_1, \dots, p_n\}$ and resulting fixed SNR vector $\vec{\gamma} = \{\bar{\gamma}_1, \dots, \bar{\gamma}_n\}$, the value s^* , for which $\mathcal{K}^{\mathbb{L}}(s, -w)$ is minimal, is determined by performing a binary search along the interval $(0, b)$, where b is the last point for which the stability condition in Eq. (10) holds. The main idea here is to cut the interval $(0, b)$ into four areas through fixing five points (see Fig. 3), where s_m is the middle point of $(0, b)$. Based on this partition, the algorithm traces the gradients and splits the range where the minimum of $\mathcal{K}^{\mathbb{L}}(s, -w)$ is located. The function is called recursively until the smallest size of an interval has been reached, defined with the input parameter

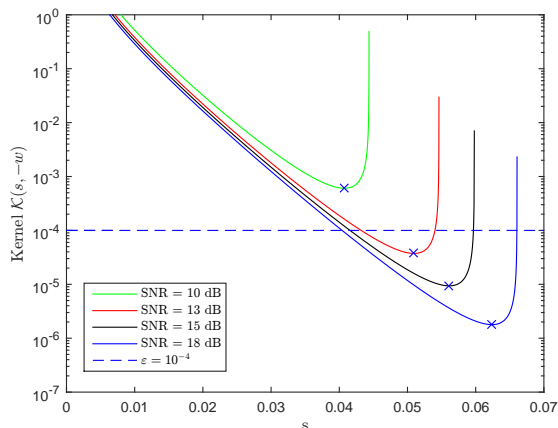


Fig. 2: The delay bound function $\mathcal{K}(s, -w)$ is convex in s . It is obtained for $r_a = 50$ bits per time slot and target delay $w = 5$ time slots. Its minimum is marked with a cross and shifts to the right as the average SNR on the link is increased.

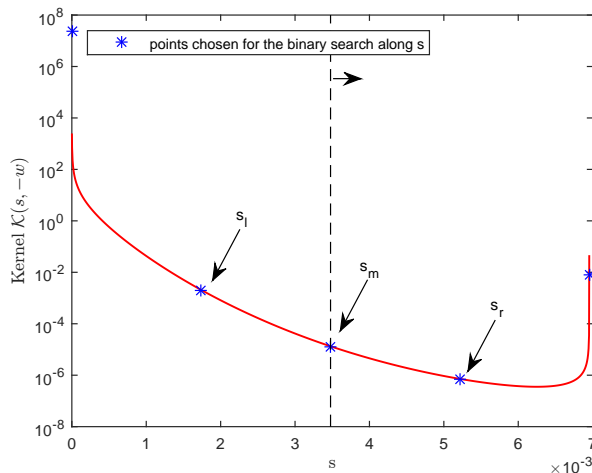


Fig. 3: The chosen points within the interval $(0, b)$ for the binary search along dimension s . s_l and s_r mark the middle of the left and right half of the interval, respectively, while s_{start} and s_{end} represent actually 0 and b , respectively.

Δ_{min} . At this point, the middle point s_m of the last considered partition is returned as s^* , i.e., as the point s for which $\mathcal{K}^{\mathcal{L}}(s, -w)$ reaches its minimum.

For the search in the second dimension along the $\vec{\gamma}$ dimension (see Algorithm 1 in Appendix B), we start by allocating a predefined maximal transmit power p_{max} to each node along the path. The link n , whose change in the transmit power results into the smallest gradient of $\mathcal{K}^{\mathcal{L}}(s^*, -w)$, $\forall n \in \{1, \dots, N\}$, is found in an iterative fashion. $\vec{\gamma}_n$ is the vector of average SNRs per link in which the n -th SNR is replaced by the SNR obtained when p_n is decreased for some predefined Δp (line 11 in Algorithm 2

Appendix B). In each iteration a new kernel is computed (denoted with $\hat{\varepsilon}$). In case the newly computed kernel is bigger than the target violation probability ε , Δp is halved, so that a decrease of the transmit power is further possible. p_n is halved until it reaches a predefined minimal value Δp_{\min} . The algorithm returns the current vector \vec{p} as an optimal one, either when all links are assigned with the maximal possible transmit power or the smallest possible Δp has been reached and the transmit power along the links cannot be further reduced. It may happen though, that the target delay cannot be met. In the optimal case the algorithm exits when the obtained kernel has approached the target violation probability from below, i.e., $\hat{\varepsilon} \in (\varepsilon - \Delta_\varepsilon, \varepsilon)$ for some predefined Δ_ε .

The obtained solution for $\vec{\gamma}$ and \vec{p} is quasi-optimal, since the binary-search algorithm approaches to the optimal s^* and the target ε . Nevertheless, the input parameters Δ_ε , Δp_{\min} and p_{\max} can be used to make a trade-off between the algorithm's precision and its performance, i.e., the needed number of iterations to reach an optimal solution.

4.2. Network Lifetime Maximization Algorithm

When having industrial automation applications in mind, reducing the transmit power results into lower interference with neighbouring networks, leading further to a better coexistence of multiple wireless technologies within the same area. However, it also increases the energy-efficiency, which is crucial for battery-powered devices in such applications. Early battery exhaustion will cause a shorter overall network lifetime as well as a potential premature network partitioning. Therefore, extending battery lifetime is another very important aspect in the performance analysis of industrial wireless applications.

We hence propose a modification of the power-minimization algorithm defined in the previous section so we can maximize network lifetime. The decision about whose link's transmit power to decrease in each iteration of the algorithm is redefined into choosing the link whose preceding node has the least charged battery at that moment of time. For this purpose we look at the battery full-states (denoted by the vector \vec{B}) of the nodes along the path \mathbb{L} . The goal is to maximize the minimal battery lifetime (or duration of battery operation) θ_n among all batteries. Each relay node can be in one of the following states: idle, send and receive. The battery consumption during the idle and the receive phase is dependent on the transceiver, while the energy consumption in the sending state is mainly dictated by the transmit power. Notice further, that the source node cannot be in receive mode, while the destination does not send packets and is therefore excluded from the decision process. Having a time slotted system with slot length T , the rest of the time slot assigned to a node, in which it neither sends nor receives the packet, is spent in an idle state.

To handle the effect described above, we formulate the following network lifetime maximization problem:

$$\begin{aligned} \max \quad & \min_{n=1 \dots N-1} \{\theta_n\}, \theta_n = \frac{B_n}{p_n \cdot T} \\ \text{s.t.} \quad & \inf\{s > 0 : \mathcal{K}^{\mathbb{L}}(s, -w^\varepsilon)\} \leq \varepsilon \\ & \max_n (\mathcal{M}_\alpha(1+s) \cdot \mathcal{M}_{g(\gamma_j)}(1-s)) < 1, \end{aligned}$$

In comparison to the gradient-based algorithm presented in Sec. 4.1, the network lifetime maximization algorithm selects the node with the minimal battery duration (the vector of battery durations is denoted by $\vec{\theta}$) as a candidate whose transmit power will be reduced in that iteration. The assigned transmit power can be selected in the interval (p_{\min}, p_{\max}) , both depending on the chosen hardware. Similar to the gradient-based algorithm, the transmit power is reduced in steps of Δp until the resulting delay bound

function (computed using Theorem 3.2) is bigger than the target one. Each time this is the case, Δp is halved until some predefined Δp_{\min} has been reached. The pseudo-code of the network lifetime algorithm is given in Algorithm 3 in Appendix B.

5. NUMERICAL EVALUATION

In this section, we present numerical evaluations of the power minimization algorithms based on the end-to-end delay bound over heterogeneous links. In Sec. 5.1 we first validate the end-to-end delay bound via simulations. In the following subsections we then focus on the power minimization algorithms. In Sec. 5.2 we evaluate our suggested algorithm for various path compositions. In Sec. 5.3 we present results that correspond to network's lifetime maximization, considering a more realistic transceiver node model in a WirelessHART network based on the IEEE 802.15.4 standard [Foundation 2013].

5.1. Validation of End-to-End Delay Bound

In this subsection we validate the end-to-end delay bound obtained from the kernel in Theorem 3.2 using simulation. We simulate a multi-hop path consisting of Rayleigh-fading channels characterized by different mean channel gains $|\bar{h}_n^2|, \forall n$. Thus, the instantaneous SNR in each time slot is exponentially distributed with mean $\bar{\gamma}_n$ per hop n . We initially consider a transmission rate equal to the Shannon capacity, leading to a service characterization per time slot i of link n given by $s_{i,n} = \log g(\gamma_{i,n}) = C \log_2(1 + \gamma_{i,n}) = \log(1 + \bar{\gamma}_n h_{i,n}^2)^C$, where again $C = C/\log 2$. The Mellin transform for the cumulative SNR service process for link n is then given by:

$\mathcal{M}_S(s, \tau, t) = \left[e^{1/\bar{\gamma}_n} \cdot \bar{\gamma}_n^{C(s-1)} \Gamma(C(s-1) + 1, 1/\bar{\gamma}_n) \right]^{t-\tau}$. For a constant arrival flow with data rate of r_a bits per time slot, the respective cumulative arrival is defined as $A(\tau, t) = r_a(t - \tau)$ and its resulting Mellin transform in the SNR domain equals $\mathcal{M}_A(s, \tau, t) = e^{r_a(t-\tau)(s-1)}$. Then the kernel for the single hop system is obtained by substituting $\bar{\gamma} = \bar{\gamma}_n$ and $\mathcal{M}_\alpha(1+s) = e^{r_a s}$ in Eq. (12), for any $s > 0$ for which the stability condition (10) holds. This kernel is subsequently used in order to obtain the end-to-end delay bound by applying Theorem 3.2.

For validation we use a fluid flow traffic model with constant rate r_a and $C = 20$ symbols per time slot. We consider both 1-hop and 3-hop paths and compare the simulated delay violation probability to our analytical results (ε) for different delay bounds w . We ran the simulation for 10^8 time slots and collected samples from the end-to-end delay of the bits departing from the last link in order to empirically characterize the delay violation probability for a given delay target. All obtained statistics are presented with a 95% confidence interval, but not always shown, due to their low absolute range.

A comparison of the analytical delay violation probability computed using Theorem 3.2 with the empirical delay violation likelihood obtained via simulation versus the target delay is depicted in Fig. 4. Here we represent 1-hop and 3-hop paths, all having the same weakest link with average SNR of 5 dB. The figure reveals that the analytical bound is indeed an upper bound to the observed system performance. An important observation is that the decay rate for the computed delay violation probability is exactly the same as that obtained via simulation which suggests that the bound is asymptotically tight. Fig. 4 further quantifies the effect of a bottleneck wireless link in a multi-hop path on the network performance and shows that it is affected by other links' qualities as well as the bottleneck link. Due to the big gap between the bottleneck link and the other links in the path with $\bar{\gamma} = \{15, 20, 5\}$ dB, this path yields almost the same performance as the 1-hop path, which is shown by both the simulation and analytical results. This observation suggests that managing the bottleneck link trans-

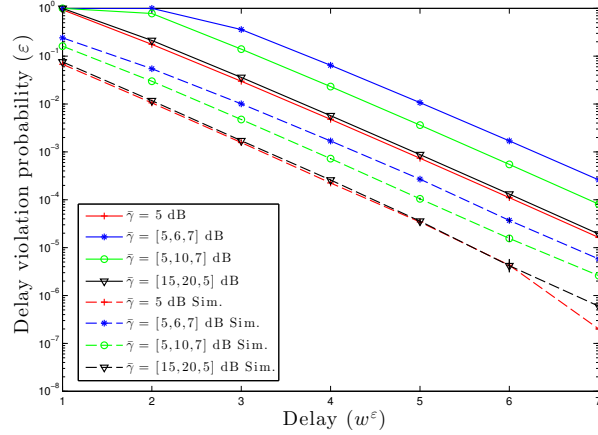


Fig. 4: Comparison of the analytical upper bound of the delay violation probability with the simulated delay violation likelihood for 1-hop and 3-hop paths with the same bottleneck link with average SNR of 5 dB. The arrival rate is $r_a = 20$ bits per time slot.

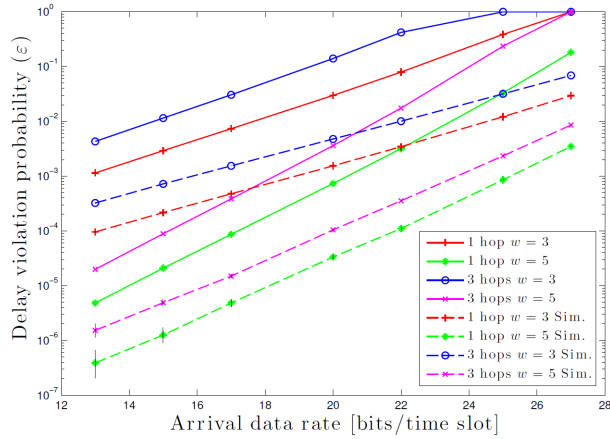


Fig. 5: Comparison of the analytical upper bound of the delay violation probability with the simulated delay violation likelihood for a one-hop path with an average SNR of 5 dB and a 3-hop path with links $[5, 10, 7]$ dB. The target delay is set to $w = \{3, 5\}$ time slots.

mit power alone (or any other link in the path) may not result in the minimum power allocation for the desired delay performance.

The analytical and simulated delay violation probability versus the arrival rate are depicted in Fig. 5. We represent here different path lengths ($N = 1$ and $N = 3$) and two different target delays ($w = 3$ and $w = 5$ time slots). The average SNR is selected to be $\bar{\gamma} = 5$ dB in the 1-hop case and $\bar{\gamma} = \{5, 10, 7\}$ dB in the 3-hop case. Obviously, for both analytical and simulation results, the violation probability increases as the target delay becomes stricter. It also increases as the path length grows. The gap between the simulated and computed curves widens for larger arrival rates, which is expected due to the use of the union bound in the computation of the delay violation probability and since violation events become more probable at high system utilization.

5.2. Evaluation of the Power-Minimization Algorithm

We now turn to the evaluation of the transmit power minimization algorithm presented in Section 4.1. Recall that the algorithm minimizes the total transmit power over all links of a multi-hop path given a target end-to-end delay violation probability ε and a target delay w .

5.2.1. Methodology. Through analytical evaluations, we benchmark the minimum total transmit power algorithm for various different scenarios, characterized by different path compositions. As in the previous subsection, we consider in general Rayleigh-fading links with different mean SNRs $\bar{\gamma}_n$. Also, we consider the Shannon capacity model as mapping from a link's SNR to its service capacity. The arrival flow in this investigation is fixed to $r_a = 20$ bits per time slot. Regarding the path compositions, we restrict ourselves in the following to paths with three hops. We express link heterogeneity for a path \mathbb{L} consisting of N links using the norm of the vector $\mathbf{l} = (l_1, \dots, l_N)$, denoted by $R^{\mathbb{L}}$ and given by:

$$R^{\mathbb{L}} = \sum_{n=1}^N \sum_{m=n+1}^N |l_n - l_m|, \quad (17)$$

where l_n denotes the length of link n , which reflects the path loss of the corresponding link and hence its service. Obviously, higher norm reflects higher link heterogeneity and vice versa. In the following, we consider 3-hop ($N = 3$) paths with various node placements between a source and a destination located 60 m apart. Table I shows the exact scenarios (from almost homogeneous to strongly heterogeneous in ascending order) and their respective path norms used in the evaluations. These scenarios are deliberately chosen to highlight the effect of link heterogeneity and relative distances between intermediate nodes on network performance and the power gain obtained using the proposed power minimization algorithm compared to a naive power allocation. Note that in the following we refer to the link with the longest distance as the *critical*

Table I: Considered Path Compositions

Link lengths in [m]	Path norm R
[20, 19, 21]	4
[20, 30, 10]	40
[5, 28, 27]	46
[20, 35, 5]	60
[5, 40, 15]	70
[5, 50.5, 4.5]	92

link (the link characterized with the highest path-loss).

In order to evaluate the efficiency of our algorithm, we are in particular interested in the total power reduction it can achieve in comparison to other approaches. For this, we consider two different comparison schemes that allocate a *uniform* power value to all links:

- *QoS-agnostic*: Each node along the path is assigned the same transmit power without considering QoS. In the numerical evaluation we use for this value the maximum available transmit power value of an IEEE 802.15.4 low-power transceiver [Corporation 2014], which equals $p_{\max} = 4$ dBm.
- *QoS-aware*: In this scheme, the transmit power is iteratively reduced equally for all nodes - starting from the maximal transmit power p_{\max} - until the obtained delay violation probability is larger than the target one (ε). Hence, as in the previous case with

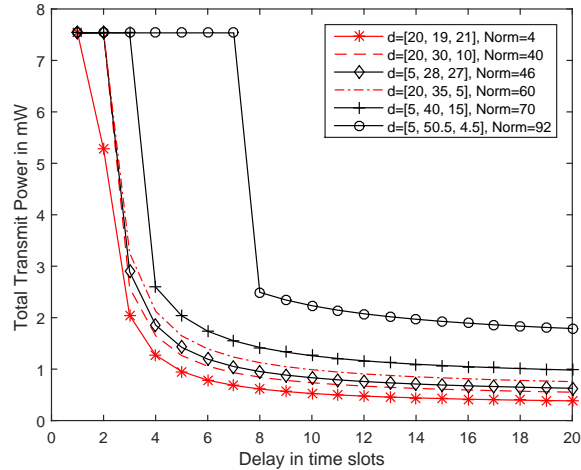


Fig. 6: Sum of the total transmit power for different 3-hop paths resulting from the power-minimization algorithm over an increasing delay target. The target delay violation probability is fixed at $\varepsilon = 10^{-3}$.

the QoS-agnostic scheme every node is assigned the same transmit power, however, the allocation is typically lower than p_{\max} .

For all considered scenarios, we compute the minimum total transmit power as obtained from our algorithm, and compute afterwards the saving ratio or the power gain (in percent) that can be obtained in comparison to the QoS-agnostic scheme or the QoS-aware scheme. A saving of 50% hence indicates that through our power minimization algorithm the total transmit power is half of the value resulting from the comparison scheme.

5.2.2. Numerical Results. In Fig. 6 we present the absolute required total transmit power in [mW] of our proposed algorithm for the discussed path scenarios over an increasing target delay when fixing the target delay violation probability. As the target delay is increased, the required total transmit power decreases. In addition, note that the total transmit power is higher for higher link heterogeneity. This is due to the critical link which dominates the total transmit power consumption on the path and for which the delay can only be compensated for by other links up to a certain point. Note that with a maximum transmit power of 4dBm per node, the total transmit power equals to 7.5357mW.

We next present the saving gains - in Fig. 7 in comparison to the QoS-agnostic scheme and in Fig. 8 in comparison to the QoS-aware scheme. For both figures we consider the same path compositions as above and vary the target delay while keeping the target delay violation probability fixed at $\varepsilon = 10^{-3}$. In Fig. 7 we observe initially that all saving gains increase for an increasing target delay. This is a direct consequence from Fig. 6, as those values are compared to a fixed value of 7.5357mW in order to determine the saving gain. Hence, it is also not surprising that the saving gain increases for more homogenous paths. In absolute terms, the saving gains are in the range of 70% to 90% which nevertheless shows the potential of the proposed algorithm.

If we switch over to the saving gains in comparison to the QoS-aware scheme different observations can be made (see Fig. 8). Now the total power consumption varies

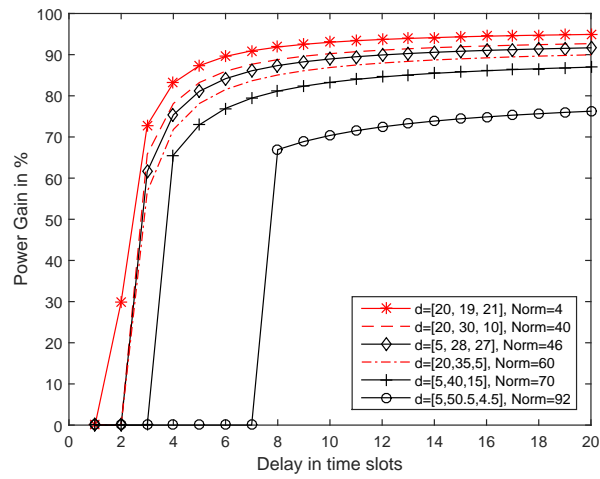


Fig. 7: Saving gain of the proposed power minimization algorithm in comparison to the QoS-agnostic scheme for an increasing target delay for various 3-hop path compositions. The target delay violation probability is fixed at $\varepsilon = 10^{-3}$.

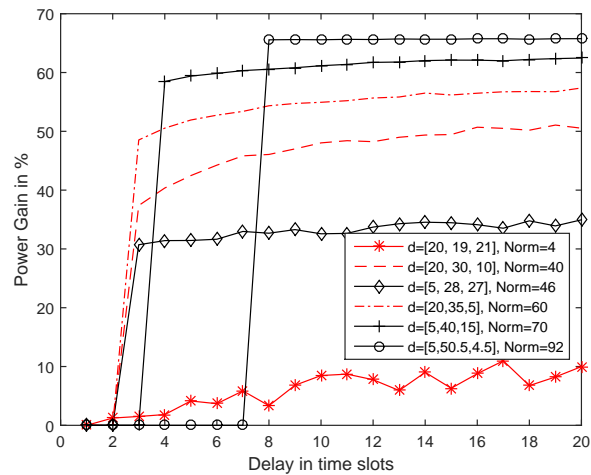


Fig. 8: Saving gain of the proposed power minimization algorithm in comparison to the QoS-aware scheme for an increasing target delay for various 3-hop path compositions. The target delay violation probability is fixed at $\varepsilon = 10^{-3}$.

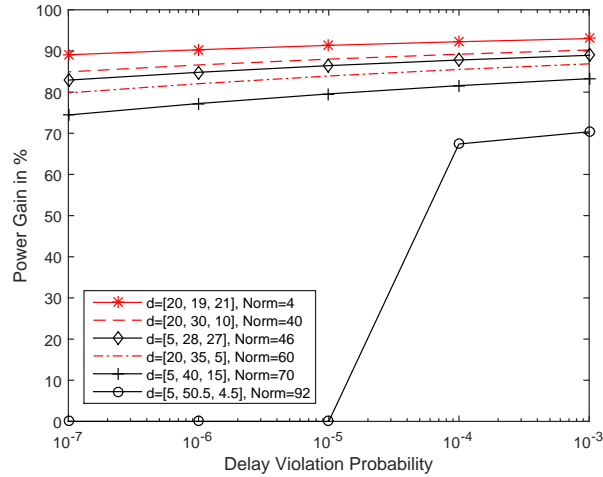


Fig. 9: Saving gain of the proposed power minimization algorithm in comparison to the QoS-agnostic scheme for an increasing target delay violation probability for various 3-hop path compositions. The target delay is fixed at $w = 10$ time slots.

as well for the comparison case, i.e., it drops in general for the larger target delays, while it also drops for paths with more homogenous link compositions, as otherwise the critical link in strongly heterogeneous paths dominates the power consumption and delay behavior. Therefore, in comparison to a QoS-agnostic comparison scheme, the proposed algorithm now provides better saving gains in case of strongly heterogeneous path compositions, as only they can be significantly exploited by the proposed algorithm. In absolute terms, this leads to saving gains in the range of 10% (in case of strongly homogeneous links) up to 70% in case of strongly heterogeneous links. Again, the power gain increases as the target delay grows.

Finally, in Fig. 9 we present the saving gain in comparison to the QoS-agnostic scheme in case of an increasing target delay violation probability for a fixed target delay of $w = 10$ time slots. We notice the same trend as in Fig. 7: The smallest saving gain is around 75% for various ε . The bigger the target violation probability, the bigger is the saving gain. Also, the more heterogeneous the paths are, the smaller is the saving gain. The path with the highest norm meets the target delay for $\varepsilon \geq 10^{-4}$ with a gain of approx. 70%.

5.3. Evaluation of the Lifetime Maximization Algorithm

We evaluate in this subsection the second proposed algorithm from Sec. 4.2, which takes the battery state of the nodes into account and maximizes the lifetime of the network by modifying the transmit power settings per node. As this scenario and objective is more relevant in practice, we also consider a more practical channel capacity in this section and resort to the WirelessHART industrial standard [Foundation 2013], widely used for process automation applications with battery-powered devices. In order to apply our proposed algorithm, we use the provided corresponding kernel given in [Petreska et al. 2016], defined according to the physical layer description and BER

stated in the IEEE 802.15.4-2006 standard [IEEE 802.15.4 WPAN Task Group 2006]³. In the following subsections we first explain our methodology and then discuss some numerical results presenting insights on how QoS-aware power management can improve network lifetime under both link and battery state heterogeneity.

5.3.1. Methodology. Let N_s be the number of time slots within a superframe, while a time slot lasts for $T = 10$ ms according to WirelessHART. We hence present the delay in number of superframes, where a superframe lasts for $T \cdot N_s$ time units. We assume a round-robin link scheduling fashion, where the n -th time slot within one superframe is assigned to the n -th link along the path, while the channel gain varies randomly in each time slot, i.e., we assume block fading.

As shown in [Petreska et al. 2016], the kernel of a single-hop WirelessHART system is given by:

$$\mathcal{K}(s, -w) = \frac{(1 + (e^{-k_a s} - 1)Q(\bar{\gamma}))^w}{1 - e^{r_a s} (1 + (e^{-k_a s} - 1)Q(\bar{\gamma}))}, \quad (18)$$

under the stability condition

$$\begin{aligned} e^{r_a s} (1 + (e^{-k_a s} - 1)Q(\bar{\gamma})) &< 1 \\ \Leftrightarrow r_a &< -\frac{1}{s} \log(1 + (e^{-k_a s} - 1)Q(\bar{\gamma})), \end{aligned} \quad (19)$$

where k_a represents the maximal number of bits that can be transmitted in a WirelessHART time slot, r_a is the size of the payload generated at the beginning of each superframe by the application and $Q(\bar{\gamma})$ is the probability of successful MAC frame transmission over the wireless link, given as a function of the BER and the average SNR [IEEE 802.15.4 WPAN Task Group 2006]. The result in Eq. (18) is explicitly derived in [Petreska et al. 2016] and serves as basis for the following numerical evaluation. The end-to-end kernel is obtained when the single-hop kernel is substituted into Theorem 3.2.

5.3.2. Numerical Results. In the following, we are mainly interested in the network lifetime extension, represented in %, obtained when applying our lifetime maximization algorithm (Algorithm 3 in Appendix B) in comparison to the QoS-agnostic scheme. The lifetime is obtained as the minimal duration a node can be operated by its corresponding battery among all node lifetimes for a given multi-hop path. The investigation is done for different target delays (in terms of superframes). We set $k_a = 127$ byte and the payload size r_a is 10 byte⁴. The arrival rate at the source node is one payload per superframe.

To parametrize the transceiver model, we turn again to the low-power Atmel IEEE802.15.4-based transceiver AT86RF233 [Corporation 2014] values that we had used above as well. The transceiver is either in idle, send or receive mode and we obtain the power consumption in these modes from the given data sheet⁵. Other system parameters are summarized in Table II.

³Note that this is no longer the active standard, since the 802.15.4-2015 is the newest version. However, the WirelessHART radios comply with IEEE 802.15.4-2006.

⁴Small packets are typical for process automation applications.

⁵Note that transceivers can offer only discrete transmit power values. Moreover, the provided data sheet contains current consumption data only for three power thresholds. For this reason, we perform polynomial curve fitting in order to obtain higher resolution consumption data and get more abstract results, not necessarily matching the transceiver capabilities in total. However, we do stay in the offered transmit power span.

Table II: System Parameters

Name	Value
Total distance	60 m
Payload size	10 byte
Frame size	127 byte
delay violation probability ε	10^{-3}
Maximal transmit power p_{\max}	4 dBm
Current consumption in idle mode	$0.2 \mu\text{A}$
Current consumption in Rx mode	11.8 mA
Time slot duration	10 ms
Time spent in Tx mode	4.256 ms
ACK duration	0.8 ms

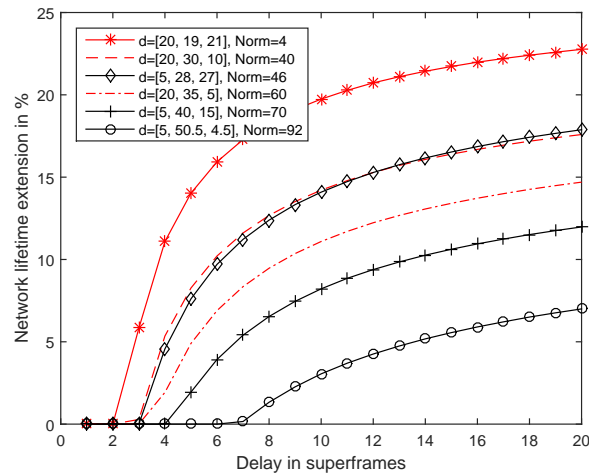


Fig. 10: Network lifetime extension for different target delays and path compositions. An equal battery state charge is assumed among all links.

For the evaluations, we again consider different multi-hop path compositions as in Table I. However, as the battery state is another important parameter regarding the efficiency of the lifetime extension algorithm, we consider in addition three settings of the battery states. In the *equal* case, the battery of each node is fully charged at the moment of algorithm execution. The *proportional* case assumes a proportional battery state distribution among the nodes regarding the path-loss on the link, i.e., the link with the highest path-loss is assigned the most charged battery. We finally consider the *inverse proportional* battery state allocation, where the link with the highest path loss is allocated the least charged battery. All presented results refer to a target delay violation probability of 10^{-3} and are compared to the QoS-agnostic power allocation scheme.

Fig. 10 shows the gain of the network lifetime extension algorithm for different delay target w considering the above discussed 3-hop path scenarios with various path norm R . In this plot, we consider the equal battery state charge among all nodes. For lower delays there is small gain in the network lifetime when using the algorithm in comparison to the QoS-agnostic scheme. As the target delay is increased, the gain in network lifetime increases. As we notice in Fig. 10, the more heterogeneous the links

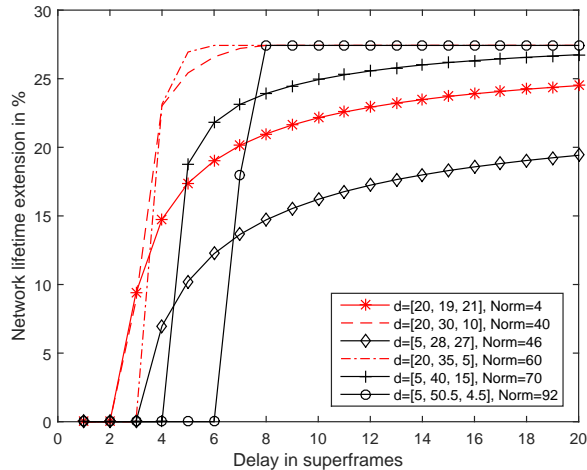


Fig. 11: Network lifetime extension for different target delays and path compositions. A proportional battery state charge is assumed among all links.

are, the less one can benefit from the proposed battery maximization algorithm. The path with the least lifetime gain is the path with link lengths $[5, 50.5, 4.5]$ m and biggest path norm.

Fig. 11 illustrates the gain in network lifetime in case of proportional initial battery state distribution. We now notice a different trend: The paths with higher link heterogeneity benefit more from the lifetime maximization algorithm than paths with lower norm. This is due to the fact that the links with lower path-loss (the better links) have a lower battery state and therefore are given advantage in the power-minimization decision, resulting finally with lower assigned transmit power and longer network lifetime. Note however, that the lowest lifetime extension is obtained for the path $[5, 28, 27]$, with the third link being the critical one (consuming the most energy, since it both sends and receives packets, in comparison to the first one).

Fig. 12 shows the network lifetime extension considering the same path scenarios for an inverse proportional initial battery state allocation, where the node in front of the weakest link is allocated the least battery capacity. We now notice the same trend as in the case of equal battery state allocation, namely that more homogeneous paths result with a larger lifetime extension. This is expected, since in both cases the algorithm prefers the links which consume more energy (i.e., the higher path-loss links) when making the decision which link's transmit power to decrease.

Finally, in Fig. 13 we show the network lifetime extension for 2-, 3- and 4-hop paths, each of them having low, moderate and high path norms. The initial battery allocation is equal among all nodes. We notice that the lifetime extension increases with the number of hops, however, still yielding the best one for paths with almost equal link path-loss, similar to the observations in Fig. 10 and Fig. 12. Hence, as the path length grows, an optimal transmit power allocation under delay constraints becomes more necessary, even for rather low link heterogeneity.

6. CONCLUSION

In this paper we provide a closed-form expression for the end-to-end delay bound in wireless heterogeneous multi-hop networks. Based on this result and using the con-

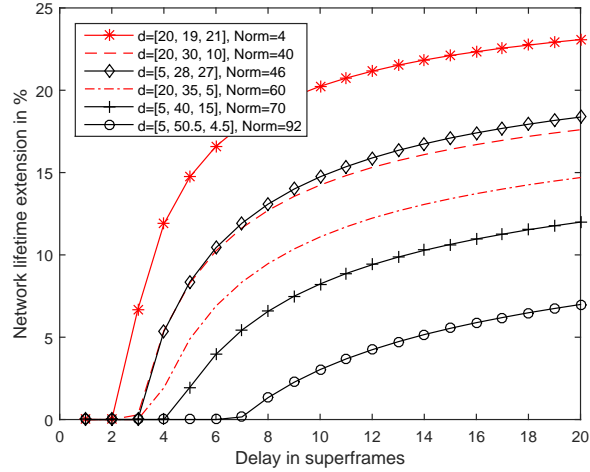


Fig. 12: Network lifetime extension for different target delays and path compositions. An inverse-proportional battery state charge is assumed among all links.

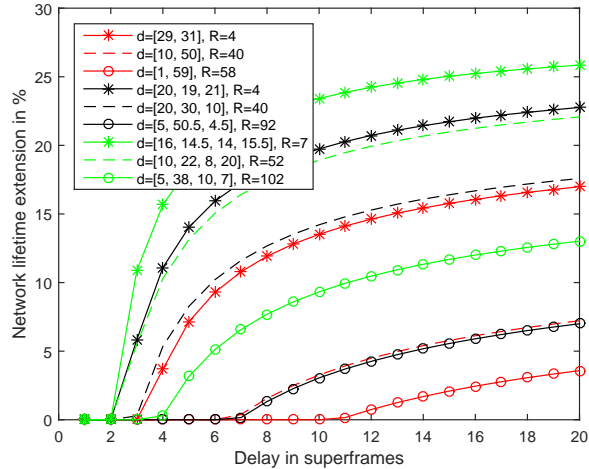


Fig. 13: Network lifetime extension for different target delays and path compositions for 2-, 3-, and 4-hop paths. An equal battery state charge is assumed among all links.

velocity of the bound, we provide a power-minimization algorithm determining the optimal transmit power per node in order to meet the end-to-end delay requirements. Two variants of the algorithm have been defined with the purpose of minimizing the total transmit power and maximizing the battery lifetime of the weakest node along the path. The provided numerical analysis covers the cases of both link and battery full-state heterogeneity and discusses in which cases delay-aware transmit power management is preferred over a static transmit power allocation scheme. In the paper we cover two service characterizations of the wireless channel: a Shannon-capacity-based

and a WirelessHART-based, applicable in real industrial systems used for process automation. The power gain obtained in the first approach yields up to 95% for almost homogeneous multi-hop paths and is bigger than 70% even for paths with highly heterogeneous links. The power gain is high even for stricter delay violation probability requirements.

The second group of numerical results shows network lifetime extension of up to 25% for various link heterogeneity and types of initial battery allocation strategies. We conclude that for nodes having equal battery capacities, the paths with higher link homogeneity benefit more of the proposed battery-lifetime maximization approach. However, in case of a different battery allocation strategy, higher lifetime extension is obtained for multi-hop paths with higher degree of link heterogeneity.

We strongly believe that the obtained results, being first such results for power-minimization over multi-hop paths with buffered, fading and heterogeneous links with delay-constrained flows, will be extremely useful for performance analysis, flow admission and network design of wireless industrial networks. The recursive nature of the provided end-to-end delay bound together with the power-minimization algorithms are a solid basis for the development of both energy-efficient and delay-aware routing algorithms in wireless multi-hop heterogeneous networks.

APPENDIX

A. DERIVATION OF THE END-TO-END DELAY BOUND

PROOF. We start by considering the bound on the Mellin transform of the service curve of path \mathbb{L} as given by Eq. (14) with $i_0 = \tau$ and $i_n = t$. Without loss of generality, let $m = n - 1$. So, we obtain:

$$\begin{aligned}
\mathcal{M}_{\mathbb{S}^{\mathbb{L}}}(s, t - \tau) &\leq \sum_{i_1, \dots, i_{n-1}}^t \prod_{j=1}^n \mathcal{M}_{g(\gamma_j)}^{i_j - i_{j-1}} \\
&= \sum_{i_1, \dots, i_{n-2}}^t \mathcal{M}_{g(\gamma_1)}^{i_1 - \tau} \mathcal{M}_{g(\gamma_2)}^{i_2 - i_1} \dots \frac{\mathcal{M}_{g(\gamma_n)}^t}{\mathcal{M}_{g(\gamma_{n-1})}^{i_{n-1} - i_{n-2}}} \sum_{i_{n-1} = i_{n-2}}^t \left(\frac{\mathcal{M}_{g(\gamma_{n-1})}}{\mathcal{M}_{g(\gamma_n)}} \right)^{i_{n-1}} \\
&= \sum_{i_1, \dots, i_{n-2}}^t \mathcal{M}_{g(\gamma_1)}^{i_1 - \tau} \cdot \mathcal{M}_{g(\gamma_2)}^{i_2 - i_1} \dots \frac{\mathcal{M}_{g(\gamma_n)}^t}{\mathcal{M}_{g(\gamma_{n-1})}^{i_{n-2}}} \\
&\quad \cdot \left(\frac{\left(\frac{\mathcal{M}_{g(\gamma_{n-1})}}{\mathcal{M}_{g(\gamma_n)}} \right)^{i_{n-2}} - \left(\frac{\mathcal{M}_{g(\gamma_{n-1})}}{\mathcal{M}_{g(\gamma_n)}} \right)^{t+1}}{1 - \frac{\mathcal{M}_{g(\gamma_{n-1})}}{\mathcal{M}_{g(\gamma_n)}}} \right) \\
&= \frac{\mathcal{M}_{g(\gamma_n)}}{\mathcal{M}_{g(\gamma_n)} - \mathcal{M}_{g(\gamma_{n-1})}} \sum_{i_1, \dots, i_{n-2}}^t \mathcal{M}_{g(\gamma_1)}^{i_1 - \tau} \dots \frac{\mathcal{M}_{g(\gamma_n)}^t}{\mathcal{M}_{g(\gamma_{n-1})}^{i_{n-2}}} \\
&\quad \cdot \left(\frac{\mathcal{M}_{g(\gamma_{n-1})}}{\mathcal{M}_{g(\gamma_n)}} \right)^{i_{n-2}} - \frac{\mathcal{M}_{g(\gamma_n)}}{\mathcal{M}_{g(\gamma_n)} - \mathcal{M}_{g(\gamma_{n-1})}} \\
&\quad \sum_{i_1, \dots, i_{n-2}}^t \mathcal{M}_{g(\gamma_1)}^{i_1 - \tau} \dots \frac{\mathcal{M}_{g(\gamma_n)}^t}{\mathcal{M}_{g(\gamma_{n-1})}^{i_{n-2}}} \left(\frac{\mathcal{M}_{g(\gamma_{n-1})}}{\mathcal{M}_{g(\gamma_n)}} \right)^t \frac{\mathcal{M}_{g(\gamma_{n-1})}}{\mathcal{M}_{g(\gamma_n)}} \\
&= \frac{\mathcal{M}_{g(\gamma_n)}}{\mathcal{M}_{g(\gamma_n)} - \mathcal{M}_{g(\gamma_{n-1})}} \sum_{i_1, \dots, i_{n-2}}^t \mathcal{M}_{g(\gamma_1)}^{i_1 - \tau} \dots \mathcal{M}_{g(\gamma_{n-2})}^{i_{n-3} - i_{n-2}} \mathcal{M}_{g(\gamma_n)}^{t - i_{n-2}}
\end{aligned}$$

$$\begin{aligned}
& - \frac{\mathcal{M}_{g(\gamma_{n-1})}}{\mathcal{M}_{g(\gamma_n)} - \mathcal{M}_{g(\gamma_{n-1})}} \sum_{i_1, \dots, i_{n-2}}^t \mathcal{M}_{g(\gamma_1)}^{i_1 - \tau} \dots \mathcal{M}_{g(\gamma_{n-2})}^{i_{n-3} - i_{n-2}} \mathcal{M}_{g(\gamma_{n-1})}^{t - i_{n-2}} \\
& = \frac{\mathcal{M}_{g(\gamma_n)}}{\mathcal{M}_{g(\gamma_n)} - \mathcal{M}_{g(\gamma_{n-1})}} \mathcal{M}_{\mathbb{S}^{\mathbb{L} \setminus \{n-1\}}} (t - \tau) \\
& + \frac{\mathcal{M}_{g(\gamma_{n-1})}}{\mathcal{M}_{g(\gamma_{n-1})} - \mathcal{M}_{g(\gamma_n)}} \mathcal{M}_{\mathbb{S}^{\mathbb{L} \setminus \{n\}}} (t - \tau),
\end{aligned}$$

where we have omitted for readability that all Mellin transforms are functions of s above. Thus, we have shown that an upper bound of the Mellin transform of path \mathbb{L} can be obtained recursively from the Mellin transform of the service process of paths $\mathbb{L} \setminus \{n-1\}$ and $\mathbb{L} \setminus \{n\}$.

As the kernel is a function of the Mellin transforms of the SNR domain arrival and service process, i.e.,

$$\mathcal{K}^{\mathbb{L}}(s, t + w, t) = \sum_{i=0}^t \mathcal{M}_{\mathcal{A}}(1 + s, i, t) \mathcal{M}_{\mathcal{S}^i}(1 - s, i, t + w),$$

it follows directly that the steady state kernel $\mathcal{K}^{\mathbb{L}}(s, -w)$ is a recursive function of the kernels $\mathcal{K}^{\mathbb{L} \setminus \{n-1\}}(s, -w)$ and $\mathcal{K}^{\mathbb{L} \setminus \{n\}}(s, -w)$ as claimed in the theorem. \square

B. PSEUDO CODES OF THE ALGORITHMS

in this appendix we present the pseudo-code for the power-minimization algorithm (Algorithm 2) and the network lifetime extension algorithm (Algorithm 3). The function *search_s* (Algorithm 1) is an auxiliary function called in both algorithms.

Algorithm 1 Search $s^* \in (0, b)$ for which $\mathcal{K}^{\mathbf{L}}(s^*, -w)$ is minimal

```

1: function SEARCH_S ( $s_{\text{start}}, b, \bar{\gamma}, \Delta_{\text{min}}, r_a, w$ )
Ensure: Find  $s^*$ 
2:   Compute  $s_1, s_m, s_r \in (s_{\text{start}}, b)$ 
3:    $s_{\text{end}} = b$ , use for simplicity  $\mathcal{K}^{\mathbf{L}}(s_i, -w) \triangleq \mathcal{K}^{\mathbf{L}}(s_i)$ 
4:   if  $s_m - s_1 > \Delta_{\text{min}}$  then
5:     Find out in which interval lies  $s^*$ 
6:     ***Case 1:  $s^* \in (s_{\text{start}}, s_m)$ 
7:     if  $\mathcal{K}^{\mathbf{L}}(s_{\text{end}}) > \mathcal{K}^{\mathbf{L}}(s_r) > \mathcal{K}^{\mathbf{L}}(s_m) > \mathcal{K}^{\mathbf{L}}(s_1)$  then
8:        $s^* = \text{search\_s}(s_{\text{start}}, s_m, \bar{\gamma}, \Delta_{\text{min}}, k_{\text{ts}}, w)$ 
9:     ***Case 2:  $s^* \in (s_m, s_{\text{end}})$ 
10:    else if  $\mathcal{K}^{\mathbf{L}}(s_{\text{start}}) > \mathcal{K}^{\mathbf{L}}(s_1) > \mathcal{K}^{\mathbf{L}}(s_m) > \mathcal{K}^{\mathbf{L}}(s_r)$  then
11:       $s^* = \text{search\_s}(s_m, s_{\text{end}}, \bar{\gamma}, \Delta_{\text{min}}, k_{\text{ts}}, w)$ 
12:    ***Case 3:  $s^* \in (s_1, s_r)$ 
13:    else if  $\mathcal{K}^{\mathbf{L}}(s_{\text{end}}) > \mathcal{K}^{\mathbf{L}}(s_r) > \mathcal{K}^{\mathbf{L}}(s_m)$ 
14:      AND  $\mathcal{K}^{\mathbf{L}}(s_{\text{start}}) > \mathcal{K}^{\mathbf{L}}(s_1) > \mathcal{K}^{\mathbf{L}}(s_m)$  then
15:         $s^* = \text{search\_s}(s_1, s_r, \bar{\gamma}, \Delta_{\text{min}}, k_{\text{ts}}, w)$ 
16:      end if
17:    else
18:       $s^* = s_m$ 
19:    return
20:  end if
21: end function

```

Algorithm 2 Power-minimization algorithm

Require: $|\vec{h}^2|, \Delta p, p_{\max}, \Delta p_{\min}, r_a, w, \varepsilon, \Delta_\varepsilon$

Ensure: $\min \sum_{n=1}^N p_n$, s.t. $\mathcal{K}^{\mathbf{L}}(s, -w) \leq \varepsilon$

- 1: $\vec{p} = p_{\max}; \bar{\gamma} = \min\{\vec{\gamma}_{\max}\} = \min[f(\vec{p}, \vec{h})]; \mathcal{K}^{\mathbf{L}}(s, -w) \triangleq \mathcal{K}^{\mathbf{L}}(s, \vec{p})$
 - 2: Find $s', \forall s \in (0, s')$, s.t. Eq. (10) holds
 - 3: Compute \vec{P}_{txmin} , s.t. channel capacity $\geq r_a$
 - 4: Compute current delay bound $\hat{\varepsilon} = \mathcal{K}^{\mathbf{L}}(s, \vec{p})$
 - 5: **if** ($\hat{\varepsilon} > \varepsilon$) **then return fail**
 - 6: **else**
 - 7: **while** ($\hat{\varepsilon} \notin (\varepsilon - \Delta_\varepsilon, \varepsilon)$) **do**
 - 8: **while** ($\hat{\varepsilon} > \varepsilon$) AND ($\Delta p \leq \Delta p_{\min}$) **do**
 - 9: Choose smaller $\Delta p : \Delta p = \Delta p/2$
 - 10: **end while**
 - 11: $\vec{p}' = \vec{p}; \vec{p}'_n$ is transmit power vector where $p_n = p'_n - \Delta p$
 - 12: Find the smallest gradient: $n = \underset{N}{\operatorname{argmin}} \nabla \mathcal{K}_n = \left| \frac{\hat{\varepsilon} - \mathcal{K}^{\mathbf{L}}(s, \vec{p}'_n)}{\Delta p} \right|$
 - 13: $p'_n = p_n - \Delta p$, assure $p'_n \geq p_{\min n}$
 - 14: $s^* = \text{search_s}(s_{\text{start}}, b, \vec{\gamma}, \Delta_{\min}, r_a, w)$; compute $\hat{\varepsilon} = \mathcal{K}^{\mathbf{L}}(s^*, \vec{p}')$
 - 15: $\vec{p} = \vec{p}'$
 - 16: **end while**
 - 17: **return** \vec{p}
 - 18: **end if**
-

Algorithm 3 Extend network lifetime

Require: $|\vec{h}^2|, \Delta p, p_{\max}, \Delta p_{\min}, k_a, r_a, w, \varepsilon, \Delta_\varepsilon, \vec{B}$

Ensure: $\max \min_m \{\theta_m\}, \theta_m \in \vec{\theta}, \vec{\theta} = \frac{\vec{B}}{T\vec{p}}, \mathcal{K}^{\mathbf{L}}(s, -w) \leq \varepsilon$

- 1: $\vec{p} = p_{\max}; \bar{\gamma} = \min\{\vec{\gamma}_{\max}\}$
 - 2: Find $s', \forall s \in (0, s')$ stability condition (10) holds
 - 3: Set P_{txmin} to transceiver capabilities; $\hat{\varepsilon} = \mathcal{K}^{\mathbf{L}}(s, -w)$
 - 4: Same approach as in Algorithm 2, only replace line 11 and 12 with
 - 5: $M = \forall m : \{\operatorname{argmin}\{\theta_m\}\}, \forall m \in M : p'_m = p_m - \frac{\Delta p}{|M|}$, assure $p'_m \geq p_{\min}$
-

C. PROOF OF THE DELAY BOUND CONVEXITY

PROOF. The delay bound (kernel) in both cases of Shannon capacity (see Eq. (12)) and WirelessHART (Eq. (18)) has the following form:

$$\begin{aligned} \mathcal{K}(s, -w) &= \frac{\mathcal{M}_{g(\gamma)}^w(1-s)}{1 - \mathcal{M}_\alpha(1+s)\mathcal{M}_{g(\gamma)}(1-s)} \\ &= \frac{(\mathcal{M}_S(1-s, \tau, t))^w}{1 - \mathcal{M}_A(1+s, \tau, t)\mathcal{M}_S(1-s, \tau, t)}, \end{aligned} \quad (20)$$

where with $\mathcal{M}_A(1+s, \tau, t)$ we define the Mellin transform of the arrival for the parameter $1+s$ and $\mathcal{M}_S(1-s, \tau, t)$ is the Mellin transform of the service process in $1-s$. According to this definition, we notice that $\mathcal{M}_A(1+s, \tau, t)$ is strictly increasing and $\mathcal{M}_S(1-s, \tau, t)$ is strictly decreasing in s . We have to prove that Eq. (20) is convex. In order to prove this, we have to prove that $\mathcal{M}_A(1+s, \tau, t) \cdot \mathcal{M}_S(1-s, \tau, t)$ is convex. If so, then $1 - \mathcal{M}_A(1+s, \tau, t) \cdot \mathcal{M}_S(1-s, \tau, t)$ is concave and $\frac{1}{1 - \mathcal{M}_A(1+s, \tau, t) \cdot \mathcal{M}_S(1-s, \tau, t)}$ and therefore Eq. (20) are convex.

Let us consider the following functions:

$$\begin{aligned} A(s) &= \mathcal{M}_A(1+s, \tau, t) = (\mathbb{E}[e^{sa}])^{t-\tau} \\ B(s) &= \mathcal{M}_S(1-s, \tau, t) = (\mathbb{E}[e^{-sc}])^{t-\tau}, \end{aligned} \quad (21)$$

where a and c are the random arrival to the link and service offered by the link. We have to prove that $A(s) \cdot B(s)$ is convex under the stability condition $A(s) \cdot B(s) < 1$. We write:

$$(\mathbb{E}[e^{sa}])^{t-\tau} (\mathbb{E}[e^{-sc}])^{t-\tau} = (\mathbb{E}[e^{-sx}])^{t-\tau} < 1, \quad (22)$$

where we substitute $x = c - a$ and use the independence of a and c . So, we have to prove that $(\mathbb{E}[e^{-sx}])^{t-\tau}$ is convex, i.e., it has to hold for any $0 \leq \theta \leq 1$ and any s in the stability interval, $s \in (0, b)$:

$$\begin{aligned} & \left(\mathbb{E}[e^{-(\theta s_1 + (1-\theta)s_2)x}] \right)^{t-\tau} \\ & \leq \theta (\mathbb{E}[e^{-s_1 x}])^{t-\tau} + (1-\theta) (\mathbb{E}[e^{-s_2 x}])^{t-\tau}. \end{aligned} \quad (23)$$

We use the Hölder inequality [Florescu and Tudor 2013]:

$$\mathbb{E}[|X \cdot Y|] \leq (\mathbb{E}|X|^p)^{1/p} \cdot (\mathbb{E}|Y|^q)^{1/q}, \quad (24)$$

for $\frac{1}{p} + \frac{1}{q} = 1$. Hence, for $\frac{1}{p} = \theta$ and $\frac{1}{q} = 1 - \theta$, we have:

$$\begin{aligned} & \left(\mathbb{E}[e^{-(\theta s_1 + (1-\theta)s_2)x}] \right)^{t-\tau} = \left(\mathbb{E}[e^{-\theta s_1 x} \cdot e^{-(1-\theta)s_2 x}] \right)^{t-\tau} \\ & \leq \left(\mathbb{E}[|e^{-\theta s_1 x}|^{1/\theta}] \right)^{(t-\tau)\theta} \cdot \left(\mathbb{E}[|e^{-(1-\theta)s_2 x}|^{1/(1-\theta)}] \right)^{(t-\tau)(1-\theta)} \\ & = (\mathbb{E}[e^{-s_1 x}])^{(t-\tau)\theta} \cdot (\mathbb{E}[e^{-s_2 x}])^{(t-\tau)(1-\theta)} \end{aligned} \quad (25)$$

If we take the exponent of the logarithm of the right hand side of Eq. (25), we obtain:

$$\begin{aligned}
& \left(\mathbb{E} \left[e^{-\left(\theta s_1 + (1-\theta) s_2 \right) x} \right] \right)^{t-\tau} \\
& \leq e^{\log \left(\left(\mathbb{E} \left[e^{-s_1 x} \right] \right)^{(t-\tau)\theta} \cdot \left(\mathbb{E} \left[e^{-s_2 x} \right] \right)^{(t-\tau)(1-\theta)} \right)} \\
& = e^{\log \theta \left(\mathbb{E} \left[e^{-s_1 x} \right] \right)^{t-\tau} + \log(1-\theta) \left(\mathbb{E} \left[e^{-s_1 x} \right] \right)^{t-\tau}} \tag{26} \\
& = \theta \left(\mathbb{E} \left[e^{-s_1 x} \right] \right)^{t-\tau} \cdot (1-\theta) \left(\mathbb{E} \left[e^{-s_2 x} \right] \right)^{t-\tau} \\
& \leq \theta \left(\mathbb{E} \left[e^{-s_1 x} \right] \right)^{t-\tau} + (1-\theta) \left(\mathbb{E} \left[e^{-s_2 x} \right] \right)^{t-\tau},
\end{aligned}$$

since it holds that $X \cdot Y \leq X + Y$, when $0 < X, Y < 1$, as $(\mathbb{E}[e^{-s_i x}])^{t-\tau} < 1, i \in \{1, 2\}$ (see Eq. (22)). Hence, we show the validity of Eq. (23), which concludes the proof on the kernel convexity.

□

REFERENCES

- Hussein Al-Zubaidy, Jörg Liebeherr, and Almut Burchard. 2013. A (min, \times) Network Calculus for Multi-Hop Fading Channels. In *IEEE Infocom*. IEEE, Turin, 1833–1841.
- S. Banerjee and Misra A. 2002. Minimum Energy Paths for Reliable Communication in Multi-hop Wireless Networks. In *MOBIHOC'02*. ACM, New York, 145–156.
- R. A. Berry. 2013. Optimal Power-Delay Tradeoffs in Fading Channels - Small-Delay Asymptotics. *IEEE Transactions on Information Theory* 59, 6 (June 2013), 3939–3952.
- Florin Ciucu. 2011. Non-Asymptotic Capacity and Delay Analysis of Mobile Wireless Networks. *SIGMETRICS Perform. Eval. Rev.* 39, 1 (June 2011), 359–360.
- Florin Ciucu, Almut Burchard, and Jörg Liebeherr. 2005. A Network Service Curve Approach for the Stochastic Analysis of Networks. In *Proceedings of the 2005 ACM SIGMETRICS International Conference on Measurement and Modeling of Computer Systems (SIGMETRICS '05)*. ACM, New York, Article 1064251, 12 pages.
- F. Ciucu, O. Hohlfeld, and Pan Hui. 2010. Non-Asymptotic Throughput and Delay Distributions in Multi-Hop Wireless Networks. In *48th Annual Allerton Conference on Communication, Control, and Computing (Allerton)*. IEEE, Illinois, 662–669.
- F. Ciucu, R. Khalili, Yuming Jiang, Liu Yang, and Yong Cui. 2014. Towards a System Theoretic Approach to Wireless Network Capacity in Finite Time and Space. In *IEEE Infocom*. IEEE, Toronto, 2391–2399.
- Francis Clarke. 2013. *Functional Analysis, Calculus of Variations and Optimal Control*. Springer-Verlag London, London, UK.
- Atmel Corporation. 2014. *MCU Wireless AT86RF233 Preliminary Datasheet*. Atmel Corporation, 1600 Technology Drive, San Jose, CA 95110 USA.
- R.L. Cruz and A.V. Santhanam. 2003. Optimal Routing, Link Scheduling and Power Control in Multi-hop Wireless Networks. In *Proc. INFOCOM 2003*. IEEE, San Francisco, 702–711.
- Brian Davies. 1978. *Integral Transforms and Their Applications*. Springer-Verlag, New York.
- M. Fidler. 2006a. An End-to-End Probabilistic Network Calculus with Moment Generating Functions. In *Quality of Service, 2006. IWQoS 2006. 14th IEEE International Workshop on*. IEEE, New Haven, CT, 261–270.
- M. Fidler. 2006b. WLC15-2: A Network Calculus Approach to Probabilistic Quality of Service Analysis of Fading Channels. In *Globecom '06. IEEE*. IEEE, San Francisco, 1–6.
- Ionut Florescu and Ciprian Tudor. 2013. *Appendix B: Inequalities Involving Random Variables and Their Expectations*. John Wiley & Sons, Inc., Wiley Online Library, 434–444. DOI : <http://dx.doi.org/10.1002/9781118593103.app2>
- HART Communications Foundation. 2013. *WirelessHART@Technology*. (2013). <http://www.hartcomm.org/>
- IEEE 802.15.4 WPAN Task Group. 2006. 802.15.4-2006 - IEEE Standard for Information technology – Local and metropolitan area networks – Specific requirements – Part 15.4: Wireless Medium Access Control (MAC) and Physical Layer (PHY) Specifications for Low Rate Wireless Personal Area Networks (WPANs). (June 2006). <https://standards.ieee.org/findstds/standard/802.15.4-2006.html>

- Y. Jiang and P.J. Emstad. 2005a. *Analysis of Stochastic Service Guarantees in Communication Networks: A Server Model*. Technical Report. Norwegian University of Science and Technology, Centre for Quantifiable Quality of Service in Communication Systems, Department of Telematics.
- Y. Jiang and P.J. Emstad. 2005b. *Analysis of Stochastic Service Guarantees in Communication Networks: A Traffic Model*. Technical Report. Norwegian University of Science and Technology, Centre for Quantifiable Quality of Service in Communication Systems, Department of Telematics.
- Yuming Jiang and Yong Liu. 2008. *Stochastic Network Calculus*. Springer, USA.
- D. Julian, Mung Chiang, D. O'Neill, and S. Boyd. 2002. QoS and Fairness Constrained Convex Optimization of Resource Allocation for Wireless Cellular and Ad Hoc Networks. In *Proc. INFOCOM 2002.*, Vol. 2. IEEE, New York, 477–486.
- S. Kandukuri and S. Boyd. 2002. Optimal Power Control in Interference-Limited Fading Wireless Channels with Outage-Probability Specifications. *IEEE Transactions on Wireless Communications* 1, 1 (Jan 2002), 46–55.
- A. V. Katsenou, E. G. Datsika, L. P. Kondi, E. Papapetrou, and K. E. Parsopoulos. 2013. Power-Aware QoS Enhancement in Multihop DS-CDMA Visual Sensor Networks. In *Digital Signal Processing (DSP), 2013 18th International Conference on*. IEEE, Fira, 1–6.
- Osama Khader and Andreas Willig. 2013. An Energy Consumption Analysis of the Wireless HART TDMA Protocol. *Computer Communications* 36, 7 (2013), 804 – 816.
- U.C. Kozat, I. Koutsopoulos, and L. Tassiulas. 2006. Cross-Layer Design for Power Efficiency and QoS Provisioning in Multi-Hop Wireless Networks. *Wireless Communications, IEEE Transactions on* 5, 11 (November 2006), 3306–3315.
- J. Lee and N. Jindal. 2009. Energy-Efficient Scheduling of Delay Constrained Traffic Over Fading Channels. *Wireless Communications, IEEE Transactions on* 8, 4 (April 2009), 1866–1875.
- R. Lubben and M. Fidler. 2012. Non-equilibrium Information Envelopes and the Capacity-Delay-Error-Tradeoff of Source Coding. In *World of Wireless, Mobile and Multimedia Networks (WoWMoM), 2012 IEEE International Symposium on a*. IEEE, San Francisco, 1–9.
- Kashif Mahmood, Mikko Vehkaperä, and Yuming Jiang. 2011. Delay Constrained Throughput Analysis of a Correlated MIMO Wireless Channel. In *Computer Communications and Networks (ICCCN), 2011 Proceedings of 20th International Conference on*. IEEE, Maui, HI, 1–7.
- M. J. Neely, E. Modiano, and C. E. Rohrs. 2005. Dynamic Power Allocation and Routing for Time-Varying Wireless Networks. *IEEE Journal on Selected Areas in Communications* 23, 1 (Jan 2005), 89–103.
- N. Petreska, H. Al-Zubaidy, and J. Gross. 2014. Power Minimization for Industrial Wireless Networks under Statistical Delay Constraints. In *Teletraffic Congress (ITC), 2014 26th International*. IEEE, Karlskrona, 1–9.
- N. Petreska, H. Al-Zubaidy, R. Knorr, and J. Gross. 2015. On the Recursive Nature of End-to-End Delay Bound for Heterogeneous Wireless Networks. In *IEEE International Conference on Communications 2015 (ICC 2015)*. IEEE, London, 5998–6004.
- N. Petreska, H. Al-Zubaidy, B. Staehle, R. Knorr, and J. Gross. 2016. Statistical Delay Bound for Wireless HART Networks. (2016). <https://arxiv.org/abs/1607.08102> to appear in Proceedings of ACM International Symposium on Performance Evaluation of Wireless Ad Hoc, Sensor and Ubiquitous Networks PE-WASUN 2016.
- J. Tang and X. Zhang. 2008a. Cross-Layer-Model Based Adaptive Resource Allocation for Statistical QoS Guarantees in Mobile Wireless Networks. *IEEE Transactions on Wireless Communications* 7, 6 (June 2008), 2318–2328.
- Jia Tang and Xi Zhang. 2008b. Power-Delay Tradeoff over Wireless Networks. In *World of Wireless, Mobile and Multimedia Networks, 2008. WoWMoM 2008. 2008 International Symposium on a*. IEEE, Newport Beach, CA, 1–12.
- Dapeng Wu and R. Negi. 2003. Effective Capacity: A Wireless Link Model for Support of Quality of Service. *IEEE Transactions Wireless Communications* 2, 4 (July 2003), 630–643.
- M. A. Zafer and E. Modiano. 2005. A Calculus Approach to Minimum Energy Transmission Policies with Quality of Service Guarantees. In *INFOCOM 2005. 24th Annual Joint Conference of the IEEE Computer and Communications Societies. Proceedings IEEE*, Vol. 1. IEEE, Miami, 548–559.
- Rong Zheng and Robin Kravets. 2005. On-demand Power Management for Ad Hoc Networks. *Ad Hoc Networks* 3, 1 (2005), 51 – 68.
- ZVEI - German Electrical and Electronic Manufacturers' Association. 2009. Coexistence of Wireless Systems in Automation Technology. (2009). <http://www.zvei.org/Publikationen/ZVEI%20Coexistence%20of%20Wireless%20Systems%20in%20Automation%20Technology.pdf>